Since January 2020 Elsevier has created a COVID-19 resource centre with free information in English and Mandarin on the novel coronavirus COVID-19. The COVID-19 resource centre is hosted on Elsevier Connect, the company's public news and information website.

Virus Research 202 (2015) 33–40

Contents lists available at ScienceDirect

Virus Research

journal homepage: www.elsevier.com/locate/virusres

New insights on the role of paired membrane structures in coronavirus replication

Philip V'kovski[a,b], Hawaa Al-Mulla[c,e], Volker Thiel[a,d,**], Benjamin W. Neuman[c,*]

[a] Federal Institute of Virology and Immunology, Mittelhäusern, Bern, Switzerland
[b] Graduate School for Biomedical Sciences, University of Bern, Switzerland
[c] School of Biological Sciences, University of Reading, Reading, Berkshire, United Kingdom
[d] Vetsuisse Faculty, University of Bern, Bern, Switzerland
[e] University of Baghdad, College of Science, Baghdad, Iraq

ARTICLE INFO

Article history:
Received 17 September 2014
Received in revised form
16 December 2014
Accepted 18 December 2014
Available online 27 December 2014

Keywords:
RNA virus replication
Membrane rearrangement
Replicative organelle
Virus factory

ABSTRACT

The replication of coronaviruses, as in other positive-strand RNA viruses, is closely tied to the formation of membrane-bound replicative organelles inside infected cells. The proteins responsible for rearranging cellular membranes to form the organelles are conserved not just among the *Coronaviridae* family members, but across the order *Nidovirales*. Taken together, these observations suggest that the coronavirus replicative organelle plays an important role in viral replication, perhaps facilitating the production or protection of viral RNA. However, the exact nature of this role, and the specific contexts under which it is important have not been fully elucidated. Here, we collect and interpret the recent experimental evidence about the role and importance of membrane-bound organelles in coronavirus replication.

1. Paired membranes associated with viral RNA

All positive-stranded RNA viruses (+RNA) that infect eukaryotes are believed to form membrane-bound replicative organelles, though this remains to be formally tested for several families of viruses (Neuman et al., 2014). One of the most widespread membrane modifications caused by +RNA viruses results in the formation of paired membranes, i.e. two closely apposed lipid bilayers. A growing body of evidence, presented in Table 1 indicates that the paired membrane structures are induced by the expression of viral proteins – most typically by parts of the viral replicase. Table 1 lists the virus lineages for which there is evidence that some form of virus-induced paired-membrane structure is associated with viral replication. The wide distribution of membrane pairing in +RNA viruses suggests that this is an effective strategy for successfully producing new viruses, and that membrane pairing may somehow increase the competitive fitness of these viruses.

While we can speculate that +RNA viruses may gain a fitness advantage by replicating on the membranes of dedicated viral organelles, this has been difficult to test experimentally. However, there are several lines of experimental and genetic evidence that suggest that RNA synthesis is tied to the formation of replicative organelles. Viral RNA accumulates in the coronavirus organelles, suggesting that the organelles may be a site of RNA synthesis (Knoops et al., 2008, 2012; Gosert et al., 2002; Hagemeijer et al., 2012). Furthermore, viral organelles are not formed when RNA synthesis is stopped (Stokes et al., 2010; Verheije et al., 2008). While it is clear that RNA synthesis is linked with the organelles, it has proved difficult to directly test whether or to what extent the process of organelle formation is necessary for the process of RNA synthesis, because of the practical difficulty in separating the two processes in an experimental setting.

2. Structure of the organelles

Electron tomography studies have revealed that the replicative organelles of different nidoviruses are drawn from a repertoire of paired-membrane structures, including (paired) convoluted membranes, pouch-like double-membrane spherules, long paired membranes and double-membrane vesicles (Knoops et al., 2008, 2012; Maier et al., 2013a), though studies of the more recently discovered mesoniviruses and roniviruses remain poorly characterized (Zirkel et al., 2011; Spann et al., 1995). The nidoviruses that have been studied to date all induced a combination

** Corresponding author at: Institute of Virology and Immunology, Längassstr.122, 3012 Bern, Switzerland. Tel.: +41 31 631 2413; fax: +41 31 631 2534.
* Corresponding author at: School of Biological Sciences, University of Reading, United Kingdom. Tel.: +44 118 378 8902.
E-mail addresses: Volker.thiel@vetsuisse.unibe.ch (V. Thiel), b.w.neuman@reading.ac.uk (B.W. Neuman).

http://dx.doi.org/10.1016/j.virusres.2014.12.021
0168-1702/

Table 1
Evidence paired membrane structures in +RNA virus infection.

Order	Family	Host[a]	Origin[b]	Type[c]	Proteins[d]	References
Nidovirales	*Arteriviridae*	A	ER	V,Z	nsp2, 3	Snijder et al. (2001), Posthuma et al. (2008), Wood et al. (1970), Pedersen et al. (1999), Pol et al. (1997)
	Coronaviridae	A	ER	V,Z,S,C	nsp3+4+6	Knoops et al. (2008), Maier et al. (2013a), Angelini et al. (2013b)
	Mesoniviridae	A	ER	V?	*nr*[e]	Thuy et al. (2013)
Picornavirales	*Picornaviridae*	A	ER	V	2BC, 3A	Hsu et al. (2010), Richards et al. (2014), Teterina et al. (1997), Suhy et al. (2000)
	Secoviridae	P	ER	V?	*nr*	Roberts and Harrison (1970)
Tymovirales	*Betaflexiviridae*	P	ER	V	*nr*	Edwardson and Christie (1978), Rudzinska-Langwald (1990)
	Tymoviridae	P	Cp, Mt	V	*nr*	Lesemann (1977)
Unclassified	*Astroviridae*	A	ER	V	nsp1a	Guix et al. (2004), Mendez et al. (2007)
	Bromoviridae	P	ER	Z,S	1a+2a^{pol}	Moreira et al. (2010), Schwartz et al. (2002), Schwartz et al. (2004)
	Closteroviridae	P	*nr*	V	*nr*	Medina et al. (1998)
	Flaviviridae	A	ER	V,S,C	NS4A+4B	Gillespie et al. (2010), Welsch et al. (2009), Romero-Brey et al. (2012), Miller et al. (2007), Roosendaal et al. (2006), Egger et al. (2002)
	Nodaviridae	A	Mito	S	pA+RNA	Kopek et al. (2010), Kopek et al. (2007)
	Togaviridae	A	Ly, ER	V,S?	P123	Magliano et al. (1998), Fontana et al. (2010), Salonen et al. (2003)
	Tombusviridae	P	Px	S	*nr*	Barajas et al. (2009)

[a] Animals (A) or Plants (P).
[b] Membranes from the endoplasmic reticulum (ER), chloroplast (Cp), mitochondria (Mt), lysosome (Ly) or peroxisome (Px).
[c] Paired membranes in the form of double-membrane vesicles (V), zippered ER (Z), open-necked spherules (S), or convoluted membranes (C).
[d] Proteins implicated in membrane rearrangements.
[e] Not reported (*nr*).

of paired-membrane features, the precise function of which have not been elucidated. It is also important to point out that to some extent the distinctions between paired membrane structures are open to interpretation and may only be fully accessible when three-dimensional imaging methods are used. A catalog of the virus-induced membrane structures that have been observed for each coronavirus is shown at right in Fig. 1.

The common element in nidovirus-like membrane rearrangement is that the membranes are paired, usually maintaining a consistent-sized gap between the two membranes (reviewed here, Angelini et al., 2014). Since protein-induced membrane

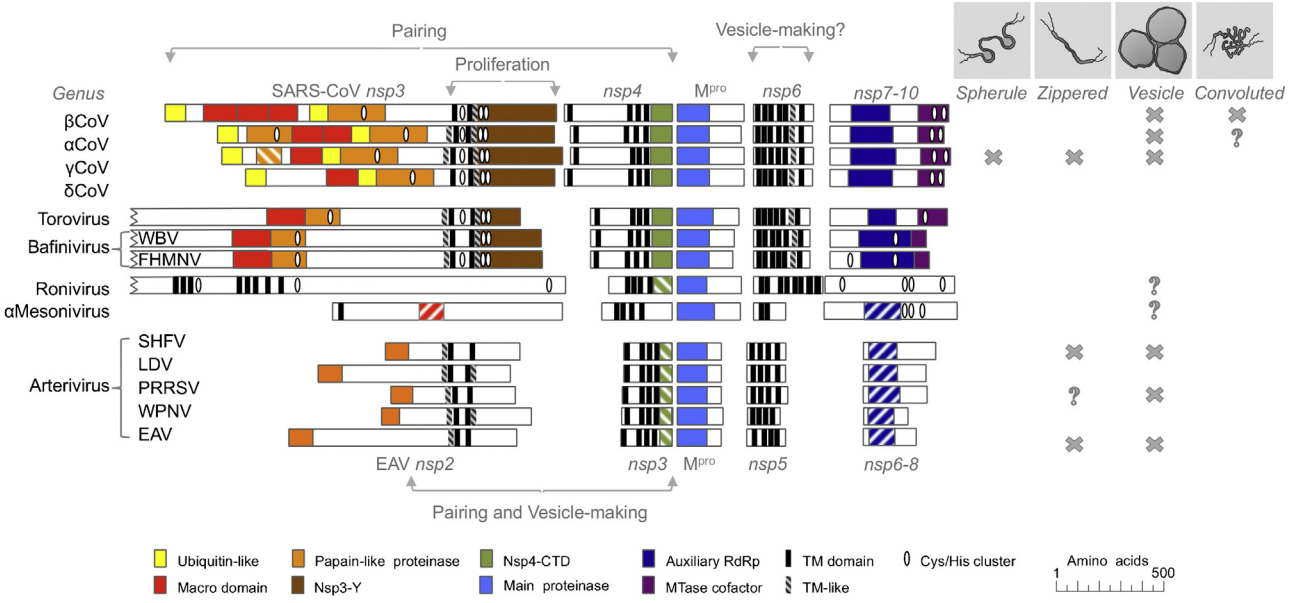

Fig. 1. Conservation and functional organization of the carboxyl-terminal region of nidovirus polyprotein 1a. Domains that are homologous at the amino acid level are shown at left in solid colors. More distantly related potential homologs identified by genome position and comparison of predicted secondary structures are marked with stripes. Positions of transmembrane regions (black bars) and hydrophobic non-transmembrane regions (striped bars) were predicted by TMHMM 2.0 (Krogh et al., 2001) and amended to reflect known topologies (Kanjanahaluethai et al., 2007; Oostra et al., 2007, 2008) wherever possible. Clusters of conserved cysteine and histidine residues that may bind metal ions are marked with white ovals. A jagged line denotes the uncertain position of the amino terminus. Regions that induce membrane pairing, proliferation or vesiculation in betacoronavirus SARS-CoV and arterivirus EAV are shown above and below the domain annotation, respectively, and all annotations come from the references listed for Table 1. Double-membrane organelles observed (x) or uncertainly observed (?) in infected cells are marked at right. Virus names are abbreviated as follows: white bream virus (WBV), fathead minnow nidovirus (FHMNV), equine arteritis virus (EAV), lactate dehydrogenase elevating virus (LDV), porcine reproductive and respiratory syndrome virus (PRRSV), simian hemorrhagic fever virus (SHFV) and wobbly possum nidovirus (WPNV).

pairing appears to be a consistent feature associated with nidovirus replication, and in the absence of data carefully dissecting the relationship between the shape and function of these different paired membrane structures, it makes sense to refer to the resulting structures collectively as double-membrane organelles (DMO).

Despite a relative wealth of structural data, it has proved difficult to test hypotheses about the role of DMOs in viral replication and fitness directly because DMO formation is linked so closely to replication and expression of replicase proteins. Here, we will discuss the implications of two recent studies that address questions about the role of DMOs in nidovirus replication (Al-Mulla et al., 2014), and characterize the effects of a new DMO-blocking drug against a variety of coronaviruses (Lundin et al., 2014).

3. Viral proteins involved in organelle formation

Further evidence of the probable importance of nidovirus replicative organelles for viral RNA replication comes in the form of genetic conservation. Nidoviruses, and most particularly coronaviruses, are highly genetically variable and contain several genus-specific or even species-specific genes (Lauber et al., 2013). However, there are two clusters of genes that are conserved in all known nidoviruses (Angelini et al., 2014; Lauber et al., 2013). The first is a highly conserved cluster of genes homologous to the Severe Acute Respiratory Syndrome Coronavirus (SARS-CoV) nsp3-6 (Fig. 1). Expression of the membrane-anchored proteins nsp3, nsp4 and nsp6 is sufficient to induce the formation of SARS-like paired-membrane replicative organelles (Angelini et al., 2013). The second conserved gene cluster encodes the viral RNA polymerase and superfamily 1 helicase (Deng et al., 2014). The conservation of membrane-pairing genes in the context of an otherwise hypervariable group of viruses is a strong argument in favor of the importance of at least the membrane-pairing genes for RNA synthesis

The proteins that form SARS-CoV replicative organelles have several features in common with distant homologs found throughout the *Nidovirales*. We will refer to the transmembrane proteins homologous to SARS-CoV nsp3, nsp4 and nsp6 a as TM1, TM2, and TM3, respectively. The relative genomic positions and functions attributed to TM1-3 in nidoviruses are shown in Fig. 1.

Of the three proteins involved in SARS-CoV replicative organelle formation, the least conserved is TM1, which has a multidomain architecture (Neuman et al., 2008). Many nidovirus and all coronavirus TM1 proteins contain one or more ubiquitin-like domains which may help to anchor the viral RNA to the membranes where replication takes place (Hurst et al., 2013). Potentially RNA-binding macrodomains (Serrano et al., 2007; Xu et al., 2009a; Wojdyla et al., 2009; Saikatendu et al., 2005; Tan et al., 2009; Chatterjee et al., 2009; Johnson et al., 2010), papain-like proteinases (Ratia et al., 2006; Wojdyla et al., 2010; van Kasteren et al., 2013), other RNA binding domains (Serrano et al., 2009) and a well conserved but poorly understood region known only as the Y domain (Neuman et al., 2008) are also commonly but not ubiquitously found in nidovirus TM1 proteins. All putative TM1 proteins are predicted to contain one or more transmembrane domains, as shown in Fig. 1. The C-terminal region of TM1, from the first transmembrane region to the end of the Y domain induces membrane proliferation, which in some ways resembles an autophagy response (Angelini et al., 2013).

TM2 and TM3 are recognizable because they contain four or more predicted transmembrane regions, and are encoded immediately before and after the viral main protease (M^{pro}). Bioinformatics generally predicts an even number of transmembrane spans in these proteins, which would be necessary to localize M^{pro} on the same side of the membrane as all of its predicted upstream and downstream cleavage sites. However there are additional hydrophobic regions that are strongly predicted to span the membrane, but which do not for several viruses, including most coronaviruses (Kanjanahaluethai et al., 2007; Oostra et al., 2007, 2008).

TM2 contains two potential conserved domains located between the first and second transmembrane domains in coronavirus, and after the final transmembrane domain in most nidoviruses. Mutations in the first non-hydrophobic domain of TM2, which is the largest part of the coronavirus replicase to localize on the luminal face of the membrane, have been demonstrated to disrupt RNA replication and may cause defects in membrane pairing (Gadlage et al., 2010). Deletion of the latter conserved domain of TM2, which has been structurally solved (Manolaridis et al., 2009; Xu et al., 2009b), was surprisingly well tolerated (Manolaridis et al., 2009; Sparks et al., 2007). TM2 localizes to membranes, but does not induce any recognizable change to intracellular membranes in the absence of other viral proteins (Angelini et al., 2013). However, co-expression of TM2 with full-length TM1 results in extensive pairing of perinuclear membranes in both coronavirus (Angelini et al., 2013) and arterivirus (Snijder et al., 2001; Posthuma et al., 2008). Additionally, it has recently been shown that co-expression of a fragment of MHV TM1 including the transmembrane region and the C-terminus with TM2 induced ER membrane zippering and curvature similar to the phenotype observed after SARS-CoV TM1 and TM2 co-expression (Hagemeijer et al., 2014). In that report TM1 and TM2 were demonstrated to interact via protein loops on the luminal face of the membrane.

The maze-like paired-membrane structures that resulted from coexpression of SARS-CoV TM1 and TM2 have not ever been reported in coronavirus-infected cells, suggesting that this should be interpreted as a conditional, or perhaps partial phenotype, that is not observed when the full viral replicase polyprotein is expressed. This suggests that membrane pairing is caused by heterotypic interactions between TM1 and TM2 on opposing membranes, but that the final architecture of the paired membranes is dependent on additional viral proteins.

TM3 largely consists of transmembrane regions, without the hallmarks of amino acid conservation or predicted structural conservation that would be expected for an enzyme. Overexpression of TM3 alone disturbs intracellular membrane trafficking (Cottam et al., 2011, 2014), resulting in an accumulation of single-membrane vesicles around the microtubule organization complex (Angelini et al., 2013). However, quantitative electron microscopy revealed that expression of TM2 with TM3 prevents the membrane disruption seen with TM3 expression alone (Angelini et al., 2013). When SARS-CoV TM1, TM2 and TM3 are coexpressed, membrane-containing bodies which resembled authentic SARS-CoV replicative organelles were formed. However, in each of the cell sections where DMV-like membranes were observed, the membrane proliferation phenotype of TM1, the paired membrane phenotype of TM1 + TM2 and the single membrane vesicle accumulation from TM3 were each visible, suggesting that these proteins do not always colocalize efficiently when expressed from plasmids in different parts of the cell instead of being expressed in the natural form as a polyprotein (BWN, personal communication). This suggests that while TM3 is not necessary for membrane pairing, TM3 may be necessary to induce the formation of the double-membrane vesicles (DMVs) that are characteristic of coronavirus replicative organelles.

4. Interactions among DMV-making proteins

The formation of large intracellular structures such as the maze-like TM1 + TM2 bodies and DMV-like TM1 + TM2 + TM3 bodies suggests that nsp3, nsp4 and nsp6 may interact both homotypically

and heterotypically. SARS-CoV nsp3–nsp3 interactions have been detected in cells by yeast two-hybridization (Pan et al., 2008) and GST pulldown (Imbert et al., 2008), and in purified protein by perfluorooctanoic acid polyacrylamide gel electrophoresis (Neuman et al., 2008). While SARS-CoV nsp4–nsp4 interactions were not found in yeast-two hybrid or mammalian two-hybrid screens (Pan et al., 2008; von Brunn et al., 2007) studies with another coronavirus did detect nsp4–nsp4 interactions by Venus reporter fluorescence (Hagemeijer et al., 2011). To date, homotypic interactions have not been demonstrated for nsp6 despite several attempts (Pan et al., 2008; Imbert et al., 2008; von Brunn et al., 2007).

Heterotypic interactions between coronavirus TM1-3 proteins have been demonstrated biochemically: a TM1–TM2 interaction was detected by mammalian two-hybridization (Pan et al., 2008) and weakly detected by Venus reporter fluorescence (Hagemeijer et al., 2011). A TM2–3 interaction has been demonstrated by Venus reporter fluorescence (Hagemeijer et al., 2011), though it did not appear in other hybridization studies. A one-way interaction between the amino-terminal 192 amino acid domain of TM1 and TM3 detected by yeast two-hybridization (Imbert et al., 2008) has also been reported. However, the apparent independence of TM1 and TM3 phenotypes after coexpression, coupled with the abrupt change in both phenotypes in the presence of TM2 suggests that interactions between these proteins may be largely mediated by TM2 (Angelini et al., 2013).

5. Virus–host interactions

Molecular interactions between host and viral factors are observed in virtually every step of the viral life cycle. Viruses rely on and manipulate established cellular pathways to accommodate their needs during replication and to counteract host innate immune signaling. Replication of coronaviruses is no exception; while some host factors have been described in the context of viral RNA replication and transcription (Zhong et al., 2012), few studies have looked closely at the complex interplay of host pathways in the establishment of virus-induced membrane-bound replication complexes.

The best available evidence suggests that most coronavirus DMO structures derive from ER membranes (Knoops et al., 2008, 2012; Maier et al., 2013a), but the precise mechanism of membrane rearrangement remains elusive. DMO membranes were initially suggested to derive from the early secretory pathway, although the absence of conventional ER, ERGIC and Golgi protein markers on viral replicative membranes argues against this hypothesis (Verheije et al., 2008; Knoops et al., 2010). Since DMVs are reminiscent of the double-membranes of autophagosomes, several lines of controversial evidence hypothesized a diversion of Atg (autophagy-related) proteins and autophagosome function during coronavirus replication, as it is the case for other +RNA viruses (Prentice et al., 2004; Snijder et al., 2006; Zhao et al., 2007; Maier and Britton, 2012; Richards and Jackson, 2013). The involvement of autophagy was recently investigated in the context of the avian CoV Infectious Bronchitis Virus (IBV) infections (Cottam et al., 2011). The authors conclude that the presence of exogenous, individually expressed IBV nsp6, which localizes to the ER, induces the formation of autophagosomes in contrast to other IBV replicase proteins. Additionally, although autophagosomes induced by IBV nsp6 or IBV infection appeared smaller than conventional autophagosomes observed after starvation of cells, they were similar in size to DMVs (Cottam et al., 2014). However, the data reported here do not appear to support the assumption that there is a functional link between IBV nsp6 and autophagosomes, and a role of the autophagy in the formation of IBV replicative structures can hereby not be demonstrated. Moreover, neither induction nor inhibition of autophagy seems to affect IBV replication (Maier et al., 2013b). It also has to be noted that the induction of autophagy by virus infection is cell type and possibly species dependent, as exemplified by the absence of LC3 puncta accumulation in IBV-infected primary chick kidney cells (Maier et al., 2013b).

New evidence concerning the source of membranes for CoV-induced DMOs was proposed, in which Mouse Hepatitis Virus (MHV) probably co-opts a cellular degradation pathway of ER-associated degradation (ERAD) regulators, known as the ERAD tuning pathway (Reggiori et al., 2010). The ERAD pathway is responsible for the turnover of folding-defective polypeptides in the ER and is modulated by stress-inducible positive regulators of ERAD-mediated protein disposal such as EDEM1 (ER degradation-enhancing alpha mannosidase-like 1) and OS-9 (osteosarcoma amplified 9). The latter assist in transporting misfolded proteins into the cytosol for subsequent degradation by the proteasomal system. Under physiological conditions, however, low concentrations of EDEM1 and OS-9 are maintained in the ER lumen in order to avoid premature degradation of proteins that are undergoing folding programs (Calì et al., 2008). In this case, EDEM1 and OS-9 are selectively confined by interacting with the transmembrane-anchored cargo receptor SEL1L (suppressor of lin-12-like protein 1) and later released from the ER lumen in small short-lived vesicles, called EDEMosomes, which rapidly fuse with the endolysosomal compartments (Bernasconi et al., 2012). This steady-state disposal of EDEM1 and OS-9 is known as ERAD tuning pathway. While not relying on the coat protein complex II (COPII) or Atg7, it critically depends on the non-lipidated form of LC3 (LC3-I), which is recruited to EDEMosomes. However, the specific autophagosomal marker GFP-LC3 does not associate with EDEMosomes, which are therefore distinct structures (Noack et al., 2014).

The coronavirus MHV is hypothesized to divert the ERAD tuning machinery for the generation of DMOs. Similarly to EDEMosomes, colocalization of EDEM1, OS-9, SEL1L, LC3-I and double-stranded (ds) RNA is observed upon MHV infection. Moreover, replication of MHV, which does not require an intact autophagy pathway, is impaired upon knockdown of LC3 or SEL1L (Bernasconi et al., 2012). DMOs furthermore lack conventional ER markers and do not associate with GFP-LC3 (Reggiori et al., 2010). Altogether, the evidence from this study may suggest that MHV exploits the ERAD-tuning machinery to establish DMOs for replication.

In order to learn whether this mechanism might be common to other nidoviruses, other viruses that use a similar replication strategy to MHV were examined. One of these, the arterivirus Equine Arteritis Virus (EAV) has been shown to require the same subset of ERAD tuning factors as MHV to ensure replication (Monastyrska et al., 2013). Recently, investigations of the even more distantly-related Japanese Encephalitis Virus (JEV), which belongs to the *Flaviviridae* family, revealed that it may usurp the same components of the ERAD-tuning pathway as well (Sharma et al., 2014). Consistent with this hypothesis, both viruses were shown to replicate independently of a functional autophagy pathway. The non-lipidated LC3 marker protein, which is essential for the replication of EAV and JEV, associated with their replication complexes together with EDEM1 whereas GFP-LC3 did not label these structures. These observations parallel the ones seen for MHV but raise further questions whether this feature is even more widespread amongst +RNA viruses.

Despite the resemblance of MHV, EAV and JEV in the requirement of host factors for efficient replication, diversion of the ERAD tuning pathway cannot be considered as a generic way of inducing replicative membranes by these viral families. Probable variations within families have to be kept in mind as exemplified by the comparison of DMOs from two different coronavirus genus members. Indeed, IBV's recently described spherules derived from paired ER membranes significantly differ from the DMO structures observed

Table 2
Differences in size and prevalence of MHV DMVs and intracellular virions (IV).

Virus	Conditions	*ts*	Cells	Prevalence				Size (nm)			
				DMV	*P* value[a]	IV	*P* value	DMV	*P* value[b]	IV	*P* value
Wild-type	DBT 33 °C	–	$n = 323$	6%	–	7%	–	228 ± 45	–	69 ± 8	–
Brts31	5.5 hpi	nsp3	$n = 753$	2%	8×10^{-4}	7%	ns[c]	195 ± 38	2×10^{-6}	69 ± 9	ns
Wild-type		–	$n = 161$	40%	–	29%	–	228 ± 36	–	68 ± 10	–
Brts31		nsp3	$n = 238$	24%	4×10^{-4}	25%	ns	208 ± 34	5×10^{-19}	68 ± 10	ns
Albts16	17Cl-1	nsp5	$n = 120$	37%	ns	19%	ns	189 ± 33	8×10^{-66}	70 ± 8	ns
Wüts18	33 °C	nsp16	$n = 140$	36%	ns	20%	ns	211 ± 35	2×10^{-15}	67 ± 12	ns
Brts105	10 hpi	nsp14	$n = 230$	22%	1×10^{-4}	32%	ns	220 ± 36	2×10^{-4}	69 ± 10	ns
Albts22[d]		nsp12	$n = 320$	13%	1×10^{-5}	9%	1×10^{-5}	204 ± 43	2×10^{-13}	68 ± 11	ns

[a] Calculated by two-tailed Fisher's exact test.
[b] Calculated by two-tailed Mann–Whitney test.
[c] Not significantly different from the appropriate wild-type control.
[d] Attenuated growth at 33 °C compared to wild-type.

upon alpha- and beta-coronaviruses infections (Maier et al., 2013a; Neuman, 2013) and their generation might require a different set of factors. Furthermore, the morphology of DMOs induced by flaviviruses such as Hepatitis C Virus, Dengue virus or West Nile Virus is highly heterogeneous and the identification of a common, conserved membrane diversion strategy seems unlikely (Romero-Brey and Bartenschlager, 2014). However, it is possible that the diversion of one pathway could lead to the generation of the different arrangements of membrane that we collectively refer to as the DMO.

Importantly, it has been shown that, in contrast to what is observed during EAV infection, endogenous LC3 does not colocalize with membrane puncta induced by expression of EAV nsp2 and nsp3, and the membrane modifications induced by the latter are not affected by LC3 knockdown (Monastyrska et al., 2013). Similarly, LC3 and EDEM1 were not recruited to rearranged membranes induced by co-expression of MHV TM1 and TM2 (Hagemeijer et al., 2014). While this still has to be proven in the context of CoV TM1, TM2 and TM3 expression, it raises the questions whether LC3 participates to the biological function of DMVs rather than its generation. A novel hypothesis has been recently suggested for Poliovirus, according to which the virus might not only co-opt a host pathway, but also divert the functional network of individual proteins (Belov and Sztul, 2014). Host factors could therefore have a proviral function during infection, distinct from the function for which they have been initially described. Accordingly, this is reminiscent with novel functions attributed to LC3 during cellular homeostasis, cytoprotection against invading pathogens or during Chlamydia trachomatis' intracellular life cycle (Bestebroer et al., 2013).

6. Natural variation in DMV structure

The DMOs of the model coronavirus MHV take the form of perinuclear DMVs which appear either singly, or grouped around and interconnected with a region of paired, convoluted membrane (CM;). A recent study examined DMV formation by *wild-type* MHV-inf-1 (*wt*) and five *temperature-sensitive* (*ts*) MHV mutants, each of which differed from *wt* by a single amino acid substitution. The panel of *ts* viruses chosen contained mutations in an interdomain linker of nsp3 (TM1), M^{pro}, the viral RNA polymerase, cap N-methyltransferase and cap O-methyltransferase, respectively (Stokes et al., 2010; Al-Mulla et al., 2014; Sawicki et al., 2005). With the exception of the polymerase mutant, which was attenuated tenfold, these viruses produced the same amount of infectious progeny as *wt* (Al-Mulla et al., 2014).

All of the mutants produced significantly smaller DMVs than *wt* virus, varying from almost *wt* size to 17% smaller (Table 2). In two of the mutants that produced normal amounts of infectious progeny, not only were the DMVs smaller, there were only about half as many DMVs per visibly infected cell compared to *wt* (Table 2). Examination of the size and number of intracellular virus particles from the same samples did not reveal corresponding changes, suggesting that the observed DMV phenotypes were not an artifact of sample preparation. The number of CMs remained in a constant ratio to the number of DMVs present, suggesting that the mutations affected production of the entire DMO.

7. Induced variation in DMVs

The DMOs of human coronavirus 229E (HCoV-229E) include DMVs similar to those observed after MHV infection (Lundin et al., 2014). In testing a new antiviral called K22, it was observed that infectivity, viral RNA, and DMV formation were all blocked by treatment with 4 μM K22. A time of addition study revealed that K22 did not block viral entry, and had the greatest antiviral effects after virus entry during the first few hours of infection, leading to the interpretation that K22 inhibits a cellular or viral component involved in a post-entry, early stage of viral replication.

After serial passage of the virus in the presence of K22, resistant mutants were selected. Surprisingly, two independently isolated resistance mutations mapped to opposite ends of transmembrane helices in TM3 (nsp6) at positions H121L and M159V. The resistant viruses released similar amounts of new progeny compared to *wt*, but produced only about half as many DMVs per infected cell. In addition, the DMVs induced by resistance mutants appeared structurally impaired. Similarly to MHV nsp4 mutants (Gadlage et al., 2010), K22 escape mutants induced DMV with partially collapsed inner membranes, even when K22 was not present. However, it is important to bear in mind that the fixation, staining and imaging conditions may have an influence on the appearance of membrane structures (Knoops et al., 2012). Moreover, the specific infectivity of those newly released virions was about tenfold lower for TM3 mutants than for wt. This suggested that the mutations in nsp6 conferred resistance to K22 at a cost of impairing an early intracellular step in the establishment of infection.

8. Fitness consequences

From these experiments it was clear that HCoV-229E viruses with K22 resistance mutations in TM3 incurred a steep fitness cost, in the form of decreased specific infectivity. There were also indications of a similar decrease in efficiency in the MHV nsp3 mutant Brts31, which produced significantly more intracellular RNA than *wt*, but without a corresponding increase in infectious progeny.

To find out if the MHV mutants also incurred a fitness cost associated with producing smaller and fewer DMVs, competitive fitness assays were carried out. To do this, equal infectivities of two viruses were added to the same flask at a temperature where both viruses could grow normally. After 24 h in direct competition, the amount of each virus was quantified either by sequencing to look for the *ts* mutation, or by phenotypically screening for *ts* and non-*ts* virus. None of the MHV mutants tested was significantly less fit than *wt* in continuous or primary fibroblasts, and two mutants were significantly fitter than *wt* under the assay conditions. One of the viruses with increased fitness compared to wild-type was the N-methyltransferase mutant Br*ts*105, which produced only half as many DMVs as *wt*. These results demonstrated that at least under these experimental conditions, producing larger or more numerous DMVs did not confer a corresponding fitness advantage.

9. Implications for coronavirus replication

When interpreting these findings, it is important to consider that none of the HCoV-229E or MHV mutants tested to date has been able to replicate entirely without DMOs. And while some of these tests were carried out in primary cells, work in animal models was not possible because of the lack of a small animal model for HCoV-229E, and because the mutations restricted the growth of MHV mutants at physiological temperatures. These two studies do not disprove the fundamental connectedness between coronavirus RNA replication and DMO formation, but together, they reveal an unexpected plasticity in the size and number of DMVs that are needed to carry out wild-type amounts of RNA synthesis.

For these reasons, along with the observation that RNA replication is detectable before the first appearance of organelles (Ulasli et al., 2010), we favor an interpretation in which the organelles are a late manifestation of accumulated viral proteins resulting from abundant RNA expression. In this interpretation, DMOs could still play an obligate role in viral replication under specific conditions or in specific cell types, but the primary role for DMOs would be to increase the efficiency of either RNA production, delivery of newly synthesized RNA to sites where it could be translated or packaged, and/or shielding abundantly synthesized viral RNA from host cell innate immune sensing pathways. These studies also suggest that at least half of the DMVs present in infected cells may be in excess of what is strictly needed to sustain normal levels of RNA synthesis, given that both MHV and HCoV-229E mutants replicated normally despite producing only half the normal complement of DMVs.

Before these studies, very little was known about the potential for natural and induced variation in intracellular membrane rearrangement. The viruses described in these studies all produced normal amounts of progeny virus particles, and were all selected for analysis for reasons unrelated to DMO formation. These represent only a handful of the available nidovirus replicase mutants that have been published. From this work we can hypothesize that other MHV *ts* mutants, or K22-resistant HCoV-229E mutants with replicase defects would probably make either smaller or fewer DMVs, and a larger collection of such mutants will like be highly informative to further our understanding on the pivotal role(s) of DMOs in the coronavirus life cycle. Hopefully the unique insight provided by these results, together with the relative ease of analysis will make quantitative electron microscopy a routine part of the characterization of new virus mutants. In addition, the accumulated knowledge on the nature of coronavirus DMOs and the possibility to experimentally interfere with DMO formation by using small compound inhibitors, such as K22, will allow us to dissect similarities and differences between viral DMOs and related cellular organelles.

The study of viral replicative organelles remains an area of active research where there are more questions than answers. For the coronavirus DMO, there are still fundamental questions that need to be answered including the roles of specific parts of the DMO in replication, the cellular pathways involved in DMO formation, and whether there are host antiviral defences that work by specifically targeting DMO formation. Some of these questions could be addressed by developing methods to study active replicase complexes and DMO membranes in vitro. There are also larger questions about the common ground in terms of membrane rearrangement and host response between coronavirus replicative organelles and those of other virus families. For now, it is clear that RNA viruses induce a variety of membrane structures that appear to have a common goal: efficiently producing progeny in the environment of an infected cell. We hope that future studies will be able to simplify this apparent complexity by separating the necessary, advantageous and dispensable components of DMO structure and function.

Acknowledgements

This work was supported by the Swiss National Science Foundation (SNF; project 149784; VT and PV) and a studentship from the Iraqi Ministry of Higher Education and Scientific Research (HA).

References

Al-Mulla, H.M., Turrell, L., Smith, N.M., Payne, L., Baliji, S., Zust, R., Thiel, V., Baker, S.C., Siddell, S.G., Neuman, B.W., 2014. Competitive fitness in coronaviruses is not correlated with size or number of double-membrane vesicles under reduced-temperature growth conditions. mBio 5, e01107–e01113.

Angelini, M.M., Akhlaghpour, M., Neuman, B.W., Buchmeier, M.J., 2013. Severe acute respiratory syndrome coronavirus nonstructural proteins 3, 4, and 6 induce double-membrane vesicles. mBio 4, e00524-00513.

Angelini, M.M., Neuman, B.W., Buchmeier, M.J., 2014. Untangling membrane rearrangement in the nidovirales. DNA Cell Biol. 33, 122–127.

Barajas, D., Jiang, Y., Nagy, P.D., 2009. A unique role for the host ESCRT proteins in replication of Tomato bushy stunt virus. PLoS Pathog. 5, e1000705.

Belov, G.A., Sztul, E., 2014. Rewiring of cellular membrane homeostasis by picornaviruses. J. Virol. 88, 9478–9489.

Bernasconi, R., Galli, C., Noack, J., Bianchi, S., de Haan, C.A., Reggiori, F., Molinari, M., 2012. Role of the SEL1L:LC3-I complex as an ERAD tuning receptor in the mammalian ER. Mol. Cell 46, 809–819.

Bestebroer, J., V'Kovski, P., Mauthe, M., Reggiori, F., 2013. Hidden behind autophagy: the unconventional roles of ATG proteins. Traffic 14, 1029–1041.

Calì, T., Galli, C., Olivari, S., Molinari, M., 2008. Segregation and rapid turnover of EDEM1 by an autophagy-like mechanism modulates standard ERAD and folding activities. Biochem. Biophys. Res. Commun. 371, 405–410.

Chatterjee, A., Johnson, M.A., Serrano, P., Pedrini, B., Joseph, J.S., Neuman, B.W., Saikatendu, K., Buchmeier, M.J., Kuhn, P., Wuthrich, K., 2009. Nuclear magnetic resonance structure shows that the severe acute respiratory syndrome coronavirus-unique domain contains a macrodomain fold. J. Virol. 83, 1823–1836.

Cottam, E.M., Maier, H.J., Manifava, M., Vaux, L.C., Chandra-Schoenfelder, P., Gerner, W., Britton, P., Ktistakis, N.T., Wileman, T., 2011. Coronavirus nsp6 proteins generate autophagosomes from the endoplasmic reticulum via an omegasome intermediate. Autophagy 7, 1335–1347.

Cottam, E.M., Whelband, M.C., Wileman, T., 2014. Coronavirus NSP6 restricts autophagosome expansion. Autophagy 10, 1426–1441.

Deng, Z., Lehmann, K.C., Li, X., Feng, C., Wang, G., Zhang, Q., Qi, X., Yu, L., Zhang, X., Feng, W., Wu, W., Gong, P., Tao, Y., Posthuma, C.C., Snijder, E.J., Gorbalenya, A.E., Chen, Z., 2014. Structural basis for the regulatory function of a complex zinc-binding domain in a replicative arterivirus helicase resembling a nonsense-mediated mRNA decay helicase. Nucl. Acids Res. 42, 3464–3477.

Edwardson, J.R., Christie, R.G., 1978. Use of virus-induced inclusions in classification and diagnosis. Ann. Rev. Phytopathol. 16, 31–55.

Egger, D., Wolk, B., Gosert, R., Bianchi, L., Blum, H.E., Moradpour, D., Bienz, K., 2002. Expression of hepatitis C virus proteins induces distinct membrane alterations including a candidate viral replication complex. J. Virol. 76, 5974–5984.

Fontana, J., Lopez-Iglesias, C., Tzeng, W.P., Frey, T.K., Fernandez, J.J., Risco, C., 2010. Three-dimensional structure of Rubella virus factories. Virology 405, 579–591.

Gadlage, M.J., Sparks, J.S., Beachboard, D.C., Cox, R.G., Doyle, J.D., Stobart, C.C., Denison, M.R., 2010. Murine hepatitis virus nonstructural protein 4 regulates virus-induced membrane modifications and replication complex function. J. Virol. 84, 280–290.

Gillespie, L.K., Hoenen, A., Morgan, G., Mackenzie, J.M., 2010. The endoplasmic reticulum provides the membrane platform for biogenesis of the flavivirus replication complex. J. Virol. 84, 10438–10447.

Gosert, R., Kanjanahaluethai, A., Egger, D., Bienz, K., Baker, S.C., 2002. RNA replication of mouse hepatitis virus takes place at double-membrane vesicles. J. Virol. 76, 3697–3708.
Guix, S., Caballero, S., Bosch, A., Pinto, R.M., 2004. C-terminal nsP1a protein of human astrovirus colocalizes with the endoplasmic reticulum and viral RNA. J. Virol. 78, 13627–13636.
Hagemeijer, M.C., Ulasli, M., Vonk, A.M., Reggiori, F., Rottier, P.J., de Haan, C.A., 2011. Mobility and interactions of coronavirus nonstructural protein 4. J. Virol. 85, 4572–4577.
Hagemeijer, M.C., Vonk, A.M., Monastyrska, I., Rottier, P.J., de Haan, C.A., 2012. Visualizing coronavirus RNA synthesis in time by using click chemistry. J. Virol. 86, 5808–5816.
Hagemeijer, M.C., Monastyrska, I., Griffith, J., van der Sluijs, P., Voortman, J., van Bergen en Henegouwen, P.M., Vonk, A.M., Rottier, P.J., Reggiori, F., de Haan, C.A., 2014. Membrane rearrangements mediated by coronavirus nonstructural proteins 3 and 4. Virology 458–459, 125–135.
Hsu, N.Y., Ilnytska, O., Belov, G., Santiana, M., Chen, Y.H., Takvorian, P.M., Pau, C., van der Schaar, H., Kaushik-Basu, N., Balla, T., Cameron, C.E., Ehrenfeld, E., van Kuppeveld, F.J., Altan-Bonnet, N., 2010. Viral reorganization of the secretory pathway generates distinct organelles for RNA replication. Cell 141, 799–811.
Hurst, K.R., Koetzner, C.A., Masters, P.S., 2013. Characterization of a critical interaction between the coronavirus nucleocapsid protein and nonstructural protein 3 of the viral replicase–transcriptase complex. J. Virol. 87, 9159–9172.
Imbert, I., Snijder, E.J., Dimitrova, M., Guillemot, J.C., Lecine, P., Canard, B., 2008. The SARS-Coronavirus PLnc domain of nsp3 as a replication/transcription scaffolding protein. Virus Res. 133, 136–148.
Johnson, M.A., Chatterjee, A., Neuman, B.W., Wuthrich, K., 2010. SARS coronavirus unique domain: three-domain molecular architecture in solution and RNA binding. J. Mol. Biol. 400, 724–742.
Kanjanahaluethai, A., Chen, Z., Jukneliene, D., Baker, S.C., 2007. Membrane topology of murine coronavirus replicase nonstructural protein 3. Virology 361, 391–401.
Knoops, K., Kikkert, M., Worm, S.H., Zevenhoven-Dobbe, J.C., van der Meer, Y., Koster, A.J., Mommaas, A.M., Snijder, E.J., 2008. SARS-coronavirus replication is supported by a reticulovesicular network of modified endoplasmic reticulum. PLoS Biol. 6, e226.
Knoops, K., Swett-Tapia, C., van den Worm, S., Te Velthuis, A., Koster, A., Mommaas, A., Snijder, E., Kikkert, M., 2010. Integrity of the early secretory pathway promotes, but is not required for, severe acute respiratory syndrome coronavirus RNA synthesis and virus-induced remodeling of endoplasmic reticulum membranes. J. Virol. 84, 833–846.
Knoops, K., Barcena, M., Limpens, R.W., Koster, A.J., Mommaas, A.M., Snijder, E.J., 2012. Ultrastructural characterization of arterivirus replication structures: reshaping the endoplasmic reticulum to accommodate viral RNA synthesis. J. Virol. 86, 2474–2487.
Kopek, B.G., Perkins, G., Miller, D.J., Ellisman, M.H., Ahlquist, P., 2007. Three-dimensional analysis of a viral RNA replication complex reveals a virus-induced mini-organelle. PLoS Biol. 5, e220.
Kopek, B.G., Settles, E.W., Friesen, P.D., Ahlquist, P., 2010. Nodavirus-induced membrane rearrangement in replication complex assembly requires replicase protein a, RNA templates, and polymerase activity. J. Virol. 84, 12492–12503.
Krogh, A., Larsson, B., von Heijne, G., Sonnhammer, E.L., 2001. Predicting transmembrane protein topology with a hidden Markov model: application to complete genomes. J. Mol. Biol. 305, 567–580.
Lauber, C., Goeman, J.J., Parquet Mdel, C., Nga, P.T., Snijder, E.J., Morita, K., Gorbalenya, A.E., 2013. The footprint of genome architecture in the largest genome expansion in RNA viruses. PLoS Pathog. 9, e1003500.
Lesemann, D.E., 1977. Virus group-specific and virus-specific cytological alterations induced by members of the tymovirus group. J. Phytopathol. 90, 315–336.
Lundin, A., Dijkman, R., Bergstrom, T., Kann, N., Adamiak, B., Hannoun, C., Kindler, E., Jonsdottir, H.R., Muth, D., Kint, J., Forlenza, M., Muller, M.A., Drosten, C., Thiel, V., Trybala, E., 2014. Targeting membrane-bound viral RNA synthesis reveals potent inhibition of diverse coronaviruses including the middle East respiratory syndrome virus. PLoS Pathog. 10, e1004166.
Magliano, D., Marshall, J.A., Bowden, D.S., Vardaxis, N., Meanger, J., Lee, J.Y., 1998. Rubella virus replication complexes are virus-modified lysosomes. Virology 240, 57–63.
Maier, H.J., Britton, P., 2012. Involvement of autophagy in coronavirus replication. Viruses 4, 3440–3451.
Maier, H.J., Hawes, P.C., Cottam, E.M., Mantell, J., Verkade, P., Monaghan, P., Wileman, T., Britton, P., 2013a. Infectious bronchitis virus generates spherules from zippered endoplasmic reticulum membranes. mBio 4, e00801–e00813.
Maier, H.J., Cottam, E.M., Stevenson-Leggett, P., Wilkinson, J.A., Harte, C.J., Wileman, T., Britton, P., 2013b. Visualizing the autophagy pathway in avian cells and its application to studying infectious bronchitis virus. Autophagy 9, 496–509.
Manolaridis, I., Wojdyla, J.A., Panjikar, S., Snijder, E.J., Gorbalenya, A.E., Berglind, H., Nordlund, P., Coutard, B., Tucker, P.A., 2009. Structure of the C-terminal domain of nsp4 from feline coronavirus. Acta Crystallogr. Sect. D Biol. Crystallogr. 65, 839–846.
Medina, V., Tian, T., Wierzchos, J., Falk, B.W., 1998. Specific inclusion bodies are associated with replication of lettuce infectious yellows virus RNAs in Nicotiana benthamiana protoplasts. J. Gen. Virol. 79 (Pt 10), 2325–2329.
Mendez, E., Aguirre-Crespo, G., Zavala, G., Arias, C.F., 2007. Association of the astrovirus structural protein VP90 with membranes plays a role in virus morphogenesis. J. Virol. 81, 10649–10658.
Miller, S., Kastner, S., Krijnse-Locker, J., Buhler, S., Bartenschlager, R., 2007. The non-structural protein 4A of dengue virus is an integral membrane protein inducing membrane alterations in a 2K-regulated manner. J. Biol. Chem. 282, 8873–8882.
Monastyrska, I., Ulasli, M., Rottier, P.J., Guan, J.L., Reggiori, F., de Haan, C.A., 2013. An autophagy-independent role for LC3 in equine arteritis virus replication. Autophagy 9, 164–174.
Moreira, A.G., Kitajima, E.W., Rezende, J.A.M., 2010. Identification and partial characterization of a Carica papaya-infecting isolate of Alfalfa mosaic virus in Brazil. J. Gen. Plant Pathol. 76, 172–175.
Neuman, B.W., 2013. How the double spherules of infectious bronchitis virus impact our understanding of RNA virus replicative organelles. mBio 4, e00987-00913.
Neuman, B.W., Joseph, J.S., Saikatendu, K.S., Serrano, P., Chatterjee, A., Johnson, M.A., Liao, L., Klaus, J.P., Yates 3rd, J.R., Wuthrich, K., Stevens, R.C., Buchmeier, M.J., Kuhn, P., 2008. Proteomics analysis unravels the functional repertoire of coronavirus nonstructural protein 3. J. Virol. 82, 5279–5294.
Neuman, B.W., Angelini, M.M., Buchmeier, M.J., 2014. Does form meet function in the coronavirus replicative organelle? Trends Microbiol. 22 (Nov(11)), 642–647, http://dx.doi.org/10.1016/j.tim.2014.06.003.
Noack, J., Bernasconi, R., Molinari, M., 2014. How viruses hijack the ERAD tuning machinery. J. Virol. 88 (Nov(18)), 10272–10275, http://dx.doi.org/10.1128/JVI.00801-14.
Oostra, M., te Lintelo, E.G., Deijs, M., Verheije, M.H., Rottier, P.J., de Haan, C.A., 2007. Localization and membrane topology of coronavirus nonstructural protein 4: involvement of the early secretory pathway in replication. J. Virol. 81, 12323–12336.
Oostra, M., Hagemeijer, M.C., van Gent, M., Bekker, C.P., te Lintelo, E.G., Rottier, P.J., de Haan, C.A., 2008. Topology and membrane anchoring of the coronavirus replication complex: not all hydrophobic domains of nsp3 and nsp6 are membrane spanning. J. Virol. 82, 12392–12405.
Pan, J., Peng, X., Gao, Y., Li, Z., Lu, X., Chen, Y., Ishaq, M., Liu, D., Dediego, M.L., Enjuanes, L., Guo, D., 2008. Genome-wide analysis of protein–protein interactions and involvement of viral proteins in SARS-CoV replication. PLoS ONE 3, e3299.
Pedersen, K.W., van der Meer, Y., Roos, N., Snijder, E.J., 1999. Open reading frame 1a-encoded subunits of the arterivirus replicase induce endoplasmic reticulum-derived double-membrane vesicles which carry the viral replication complex. J. Virol. 73, 2016–2026.
Pol, J.M., Wagenaar, F., Reus, J.E., 1997. Comparative morphogenesis of three PRRS virus strains. Vet. Microbiol. 55, 203–208.
Posthuma, C.C., Pedersen, K.W., Lu, Z., Joosten, R.G., Roos, N., Zevenhoven-Dobbe, J.C., Snijder, E.J., 2008. Formation of the arterivirus replication/transcription complex: a key role for nonstructural protein 3 in the remodeling of intracellular membranes. J. Virol. 82, 4480–4491.
Prentice, E., Jerome, W., Yoshimori, T., Mizushima, N., Denison, M., 2004. Coronavirus replication complex formation utilizes components of cellular autophagy. J. Biol. Chem. 279, 10136–10141.
Ratia, K., Saikatendu, K.S., Santarsiero, B.D., Barretto, N., Baker, S.C., Stevens, R.C., Mesecar, A.D., 2006. Severe acute respiratory syndrome coronavirus papain-like protease: structure of a viral deubiquitinating enzyme. Proc. Natl. Acad. Sci. U. S. A. 103, 5717–5722.
Reggiori, F., Monastyrska, I., Verheije, M.H., Cali, T., Ulasli, M., Bianchi, S., Bernasconi, R., de Haan, C.A., Molinari, M., 2010. Coronaviruses Hijack the LC3-I-positive EDEMosomes, ER-derived vesicles exporting short-lived ERAD regulators, for replication. Cell Host Microbe 7, 500–508.
Richards, A.L., Jackson, W.T., 2013. How positive-strand RNA viruses benefit from autophagosome maturation. J. Virol. 87, 9966–9972.
Richards, A.L., Soares-Martins, J.A., Riddell, G.T., Jackson, W.T., 2014. Generation of unique poliovirus RNA replication organelles. mBio 5, e00833-00813.
Roberts, I.M., Harrison, B.D., 1970. Inclusion bodies and tubular structures in Chenopodium amaranticolor plants infected with strawberry latent ringspot virus. J. Gen. Virol. 7, 47–54.
Romero-Brey, I., Bartenschlager, R., 2014. Membranous replication factories induced by plus-strand RNA viruses. Viruses 6, 2826–2857.
Romero-Brey, I., Merz, A., Chiramel, A., Lee, J.Y., Chlanda, P., Haselman, U., Santarella-Mellwig, R., Habermann, A., Hoppe, S., Kallis, S., Walther, P., Antony, C., Krijnse-Locker, J., Bartenschlager, R., 2012. Three-dimensional architecture and biogenesis of membrane structures associated with hepatitis C virus replication. PLoS Pathog. 8, e1003056.
Roosendaal, J., Westaway, E.G., Khromykh, A., Mackenzie, J.M., 2006. Regulated cleavages at the West Nile virus NS4A-2K-NS4B junctions play a major role in rearranging cytoplasmic membranes and Golgi trafficking of the NS4A protein. J. Virol. 80, 4623–4632.
Rudzinska-Langwald, A., 1990. Cytological changes in phloem parenchyma cells of Solanum rostratum (Dunal.) related to the replication of potato virus M (PVM). Acta Soc. Bot. Pol. 59, 45–53.
Saikatendu, K.S., Joseph, J.S., Subramanian, V., Clayton, T., Griffith, M., Moy, K., Velasquez, J., Neuman, B.W., Buchmeier, M.J., Stevens, R.C., Kuhn, P., 2005. Structural basis of severe acute respiratory syndrome coronavirus ADP-ribose-1″-phosphate dephosphorylation by a conserved domain of nsP3. Structure 13, 1665–1675.
Salonen, A., Vasiljeva, L., Merits, A., Magden, J., Jokitalo, E., Kaariainen, L., 2003. Properly folded nonstructural polyprotein directs the semliki forest virus replication complex to the endosomal compartment. J. Virol. 77, 1691–1702.
Sawicki, S.G., Sawicki, D.L., Younker, D., Meyer, Y., Thiel, V., Stokes, H., Siddell, S.G., 2005. Functional and genetic analysis of coronavirus replicase-transcriptase proteins. PLoS Pathogens 1, e39.

Schwartz, M., Chen, J., Janda, M., Sullivan, M., den Boon, J., Ahlquist, P., 2002. A positive-strand RNA virus replication complex parallels form and function of retrovirus capsids. Mol. cell 9, 505–514.

Schwartz, M., Chen, J., Lee, W.M., Janda, M., Ahlquist, P., 2004. Alternate, virus-induced membrane rearrangements support positive-strand RNA virus genome replication. Proc. Natl. Acad. Sci. U. S. A. 101, 11263–11268.

Serrano, P., Johnson, M.A., Almeida, M.S., Horst, R., Herrmann, T., Joseph, J.S., Neuman, B.W., Subramanian, V., Saikatendu, K.S., Buchmeier, M.J., Stevens, R.C., Kuhn, P., Wuthrich, K., 2007. Nuclear magnetic resonance structure of the N-terminal domain of nonstructural protein 3 from the severe acute respiratory syndrome coronavirus. J. Virol. 81, 12049–12060.

Serrano, P., Johnson, M.A., Chatterjee, A., Neuman, B.W., Joseph, J.S., Buchmeier, M.J., Kuhn, P., Wuthrich, K., 2009. Nuclear magnetic resonance structure of the nucleic acid-binding domain of severe acute respiratory syndrome coronavirus nonstructural protein 3. J. Virol. 83, 12998–13008.

Sharma, M., Bhattacharyya, S., Nain, M., Kaur, M., Sood, V., Gupta, V., Khasa, R., Abdin, M., Vrati, S., Kalia, M., 2014. Japanese encephalitis virus replication is negatively regulated by autophagy and occurs on LC3-I- and EDEM1-containing membranes. Autophagy 10, 53–153.

Snijder, E.J., van Tol, H., Roos, N., Pedersen, K.W., 2001. Non-structural proteins 2 and 3 interact to modify host cell membranes during the formation of the arterivirus replication complex. J. Gen. Virol. 82, 985–994.

Snijder, E., van der Meer, Y., Zevenhoven-Dobbe, J., Onderwater, J., van der Meulen, J., Koerten, H., Mommaas, A., 2006. Ultrastructure and origin of membrane vesicles associated with the severe acute respiratory syndrome coronavirus replication complex. J. Virol. 80, 5927–5940.

Spann, K.M., Vickers, J.E., Lester, R.J.G., 1995. Lymphoid organ virus of *Penaeus monodon* from Australia. Dis. Aquat. Org. 23, 127–134.

Sparks, J.S., Lu, X., Denison, M.R., 2007. Genetic analysis of Murine hepatitis virus nsp4 in virus replication. J. Virol. 81, 12554–12563.

Stokes, H.L., Baliji, S., Hui, C.G., Sawicki, S.G., Baker, S.C., Siddell, S.G., 2010. A new cistron in the murine hepatitis virus replicase gene. J. Virol. 84, 10148–10158.

Suhy, D.A., Giddings Jr., T.H., Kirkegaard, K., 2000. Remodeling the endoplasmic reticulum by poliovirus infection and by individual viral proteins: an autophagy-like origin for virus-induced vesicles. J. Virol. 74, 8953–8965.

Tan, J., Vonrhein, C., Smart, O.S., Bricogne, G., Bollati, M., Kusov, Y., Hansen, G., Mesters, J.R., Schmidt, C.L., Hilgenfeld, R., 2009. The SARS-unique domain (SUD) of SARS coronavirus contains two macrodomains that bind G-quadruplexes. PLoS Pathog. 5, e1000428.

Teterina, N.L., Bienz, K., Egger, D., Gorbalenya, A.E., Ehrenfeld, E., 1997. Induction of intracellular membrane rearrangements by HAV proteins 2C and 2BC. Virology 237, 66–77.

Thuy, N.T., Huy, T.Q., Nga, P.T., Morita, K., Dunia, I., Benedetti, L., 2013. A new nidovirus (NamDinh virus NDiV): its ultrastructural characterization in the C6/36 mosquito cell line. Virology 444, 337–342.

Ulasli, M., Verheije, M.H., de Haan, C.A., Reggiori, F., 2010. Qualitative and quantitative ultrastructural analysis of the membrane rearrangements induced by coronavirus. Cell. Microbiol. 12, 844–861.

van Kasteren, P.B., Bailey-Elkin, B.A., James, T.W., Ninaber, D.K., Beugeling, C., Khajehpour, M., Snijder, E.J., Mark, B.L., Kikkert, M., 2013. Deubiquitinase function of arterivirus papain-like protease 2 suppresses the innate immune response in infected host cells. Proc. Natl. Acad. Sci. U. S. A. 110, E838–E847.

Verheije, M.H., Raaben, M., Mari, M., Te Lintelo, E.G., Reggiori, F., van Kuppeveld, F.J., Rottier, P.J., de Haan, C.A., 2008. Mouse hepatitis coronavirus RNA replication depends on GBF1-mediated ARF1 activation. PLoS Pathog. 4, e1000088.

von Brunn, A., Teepe, C., Simpson, J.C., Pepperkok, R., Friedel, C.C., Zimmer, R., Roberts, R., Baric, R., Haas, J., 2007. Analysis of intraviral protein–protein interactions of the SARS coronavirus ORFeome. PLoS ONE 2, e459.

Welsch, S., Miller, S., Romero-Brey, I., Merz, A., Bleck, C.K., Walther, P., Fuller, S.D., Antony, C., Krijnse-Locker, J., Bartenschlager, R., 2009. Composition and three-dimensional architecture of the dengue virus replication and assembly sites. Cell Host Microbe 5, 365–375.

Wojdyla, J.A., Manolaridis, I., Snijder, E.J., Gorbalenya, A.E., Coutard, B., Piotrowski, Y., Hilgenfeld, R., Tucker, P.A., 2009. Structure of the X (ADRP) domain of nsp3 from feline coronavirus. Acta Crystallogr. Sect. D Biol. Crystallogr. 65, 1292–1300.

Wojdyla, J.A., Manolaridis, I., van Kasteren, P.B., Kikkert, M., Snijder, E.J., Gorbalenya, A.E., Tucker, P.A., 2010. Papain-like protease 1 from transmissible gastroenteritis virus: crystal structure and enzymatic activity toward viral and cellular substrates. J. Virol. 84, 10063–10073.

Wood, O., Tauraso, N., Liebhaber, H., 1970. Electron microscopic study of tissue cultures infected with simian haemorrhagic fever virus. J. Gen. Virol. 7, 129–136.

Xu, Y., Cong, L., Chen, C., Wei, L., Zhao, Q., Xu, X., Ma, Y., Bartlam, M., Rao, Z., 2009a. Crystal structures of two coronavirus ADP-ribose-1″-monophosphatases and their complexes with ADP-Ribose: a systematic structural analysis of the viral ADRP domain. J. Virol. 83, 1083–1092.

Xu, X., Lou, Z., Ma, Y., Chen, X., Yang, Z., Tong, X., Zhao, Q., Xu, Y., Deng, H., Bartlam, M., Rao, Z., 2009b. Crystal structure of the C-terminal cytoplasmic domain of non-structural protein 4 from mouse hepatitis virus A59. PLoS ONE 4, e6217.

Zhao, Z., Thackray, L., Miller, B., Lynn, T., Becker, M., Ward, E., Mizushima, N., Denison, M., Virgin, H., 2007. Coronavirus replication does not require the autophagy gene ATG5. Autophagy 3, 581–585.

Zhong, Y., Tan, Y.W., Liu, D.X., 2012. Recent progress in studies of arterivirus– and coronavirus–host interactions. Viruses 4, 980–1010.

Zirkel, F., Kurth, A., Quan, P.L., Briese, T., Ellerbrok, H., Pauli, G., Leendertz, F.H., Lipkin, W.I., Ziebuhr, J., Drosten, C., Junglen, S., 2011. An insect nidovirus emerging from a primary tropical rainforest. mBio 2 (3), e00077-11.